

Mutations to *R. sphaeroides* Reaction Center Perturb Energy Levels and Vibronic Coupling but Not Observed Energy Transfer Rates

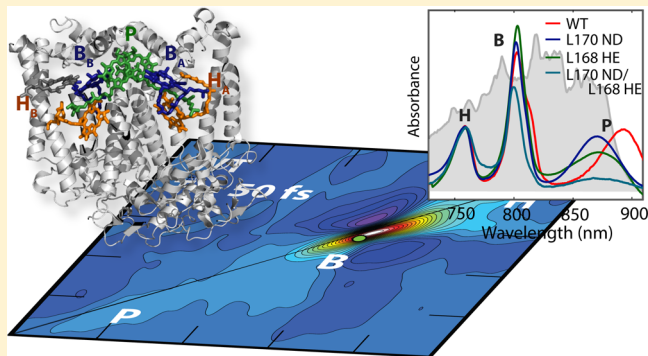
Moira L. Flanagan,[†] Phillip D. Long,[†] Peter D. Dahlberg,[†] Brian S. Rolczynski,[‡] Sara C. Massey,[‡] and Gregory S. Engel^{*‡}

[†]Graduate Program in the Biophysical Sciences, The James Franck Institute and The Institute for Biophysical Dynamics, The University of Chicago, Chicago, Illinois 60637, United States

[‡]Department of Chemistry, The James Franck Institute and The Institute for Biophysical Dynamics, The University of Chicago, Chicago, Illinois 60637, United States

Supporting Information

ABSTRACT: The bacterial reaction center is capable of both efficiently collecting and quickly transferring energy within the complex; therefore, the reaction center serves as a convenient model for both energy transfer and charge separation. To spectroscopically probe the interactions between the electronic excited states on the chromophores and their intricate relationship with vibrational motions in their environment, we examine coherences between the excited states. Here, we investigate this question by introducing a series of point mutations within 12 Å of the special pair of bacteriochlorophylls in the *Rhodobacter sphaeroides* reaction center. Using two-dimensional spectroscopy, we find that the time scales of energy transfer dynamics remain unperturbed by these mutations. However, within these spectra, we detect changes in the mixed vibrational-electronic coherences in these reaction centers. Our results indicate that resonance between bacteriochlorophyll vibrational modes and excitonic energy gaps promote electronic coherences and support current vibronic models of photosynthetic energy transfer.



I. INTRODUCTION

Photosynthetic organisms collect light with pigment–protein complexes and then funnel the energy to a reaction center for charge separation prior to downstream biochemistry that stores it in chemical form. This energy transfer can be extraordinarily fast and efficient, but it still is not fully understood.^{1–5} Many studies have excited coherences between electronic and vibronic states and observed that such coherences can persist on the time scales of energy transfer, suggesting that coherent relaxation mechanisms may be important for energy transfer. It has been suggested that the protein creates a local environment protecting chromophores and coherences from external environmental fluctuations.^{6,7} Alternatively, the dynamics may be properties of the chromophores as the electronic states interact with vibrational motions of the chromophores themselves.⁸ Bacteriochlorophylls are distinctive chromophores with multiple strong transition dipoles, established solvatochromatic dependence on their environment, and a complicated vibrational structure.^{9,10} Does the robustness of energy transfer come from the protein environment or is it intrinsic to the chromophore? To address this question, we first perturb the protein environment on the amino acid level, and then we specifically consider ramifications on the nearby chromophores. We present cryogenic two-dimensional electronic spectroscopy (2DES)^{11–13} data for several mutants of the reaction center

(RC) from *Rhodobacter sphaeroides*. Two amino acids near the special pair pocket are mutated to charged residues, and the cryogenic temperature narrows features so they are distinguishable. We present and analyze the resulting dynamics and coherences present in these complexes.

The connection between coherences and energy transfer is not yet fully understood. In 2DES, coherences have both electronic and vibrational origins.^{6,8,14–28} For the sake of clarity, we will use the term vibronic to refer to any mixing between electronic and vibrational degrees of freedom. At the most fundamental level, observed coherences report on how the electronic system interacts with the surrounding environment. The coherence lifetime indicates how well memory is preserved in the system. It is unclear how sensitive light-harvesting dynamics is to a specific amino acid sequence.^{16,29} Coherences act as a tool to characterize the changes to the environment due to these mutations. They allow us to correlate changes in the system–bath interactions to changes in transport dynamics.

Special Issue: James G. Anderson Festschrift

Received: August 27, 2015

Revised: December 1, 2015

Published: December 2, 2015



In this work, we employ the RC as a model for energy transfer in a photosynthetic system. However, the RC exists *in vivo* primarily as the charge separation complex. We chose this complex because, in contrast to many light-harvesting antenna complexes that have congested spectra involving many chromophores, the reaction center exhibits three well-separated absorption peaks in the far-red and near-IR electromagnetic spectrum termed P, B, and H (Figure 1). Energy transfer among these spectral bands has been well-studied.^{2–4,9} In this work, we alter the immediate environment around the special pair by amino acid point mutations. If the energy transfer and coupling between the chromophores depend on the amino acid contribution to the bath, we expect to see changes in rates or coupling to the environment with these mutations. We then further investigate the resonance between vibrational and electronic transitions to understand the design principles of solar light harvesting.

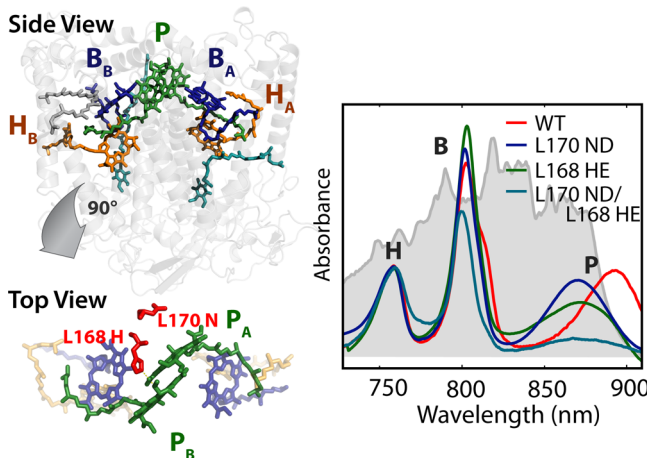


Figure 1. *R. sphaeroides* reaction center complex mutants' structure and absorption spectra. The protein backbone contains the chromophores inside the matrix. With our bandwidth (gray shading), we can access the Q_y transitions of the two bacteriochlorophyll bands, B and P, and the bacteriopheophytin band, H. The absorption spectra of the wild type (WT) and three mutants (L170ND, L168HE, L170ND/L168HE) are shown. The mutations around the tightly coupled special pair (P) blue shift the P feature.

II. EXPERIMENTAL SECTION

A. Sample Preparation. The wild-type and mutant reaction centers were polyhistidine-tagged and isolated from *R. sphaeroides* according to established protocols.³⁰ Cells were grown semiaerobically at 31 °C, lysed by sonication, solubilized in 0.1% LDAO and purified with a Ni-NTA resin column, with a final buffer of 10 mM Tris, 0.1% LDAO, and 10 mM NaCl at pH 7.0. The sample was mixed to 50% glycerol, with a final optical density (OD) of 0.3 at 800 nm in a 0.2 mm silanized quartz cell and quickly cooled to 77 K with an Oxford Instruments liquid nitrogen cryostat. Immediately before freezing, ~100 mM sodium ascorbate was added to all samples.

B. Spectroscopy. Two-dimensional electronic spectroscopy was performed as described in previous publications.^{31,32} Three beams are focused on a common point on the sample producing a signal in the phase-matched direction $k_s = -k_1 + k_2 + k_3$. For each 2D spectrum, the first time interval, the coherence time, is scanned from −0 to +200 at 4 fs intervals acquiring only the rephasing Feynmann pathways. Waiting times

were scanned from −100 to +1000 fs in 5 fs intervals. At the sample, each beam was 5–10 nJ/pulse, 8–12 fs in temporal length, and focused to a 90 μm beam waist for all the experiments. A representative broadband laser spectrum is shown in Figure 1. All data are phased to separately acquired pump–probe data (Figure S8).³³ The broader bandwidth accesses more complete context for the observed dynamics. However, the broader bandwidth spectrum was achieved at cost to laser power stability (0.4% to 0.9% standard deviation (SD)/mean; 10 Hz), so replicate data for each sample with narrower bandwidth and more stable laser power (0.1–0.4% SD/mean) are shown in the Supporting Information to verify the accuracy of our observations.

III. RESULTS

A. Spectroscopy of Mutant Reaction Centers. The cryogenic linear absorption spectrum of each reaction center mutant is shown in Figure 1 with labeled P, B, and H peaks. Each spectrum in Figure 1 is normalized to the H peak because the bacteriopheophytins are least affected by our mutations. Each of the three peaks can be assigned principally to a pair of specific chromophores. The P, B, and H peaks are composed primarily of the special pair, accessory bacteriochlorophyll, and bacteriopheophytins, respectively. These six chromophores are arranged in two nearly symmetric branches within the protein scaffold. Energy transfer occurs downhill in energy from H toward P.⁹ The P and B peaks are each composed of two bacteriochlorophylls, yet the two bands absorb at different frequencies. The strong coupling between the two closely spaced P chromophores creates strong excitonic mixing, and the geometry dictates that the lower energy band will carry the oscillator strength, giving rise to the strong red shift of the P-band. The higher energy excitonic band of the special pair (P^+) absorbs weakly between 810 and 840 nm and appears as a slight shoulder on the B peak in the linear absorption spectrum.³ Therefore, we attribute the differences in the intensity of the B peak in Figure 1 largely to changes in the P absorption due to mutation.

We study four reaction center variants: the wild-type RC, RCs with one of two different point mutations, L170ND and L168HE, and a double mutant with both mutations. The L170ND mutation replaces an asparagine residue approximately 12 Å from the special pair with an aspartic acid. The L168HE mutation represents an even more drastic change, removing a hydrogen bond attaching the special pair to the protein. The special pair is where charge transfer in bacterial photosynthesis is initiated. These mutations are known to disrupt charge transfer in this complex and have been studied in this capacity previously.³⁴ In this work, the samples are in reduced conditions to minimize any long-lived charge transfer state and we investigate the effect of these perturbations on energy transfer and interpigment coupling. These mutations each blue shift the P peak relative to the wild type (WT), but we do not see a significant red shift of the P^+ band. The absorption spectrum of a chromophore tends to red shift when its environment changes from solution to a protein cavity. The blue shift in the mutants reveals a decoupling of the special pair to the protein matrix³⁴ without significantly altering the coupling between the P chromophores. The broadening of the P absorption band, especially noticeable in the L168HE mutant and the double mutant, is consistent with an increase in heterogeneity across the ensemble implying that the special pair is somewhat destabilized without this hydrogen bond.

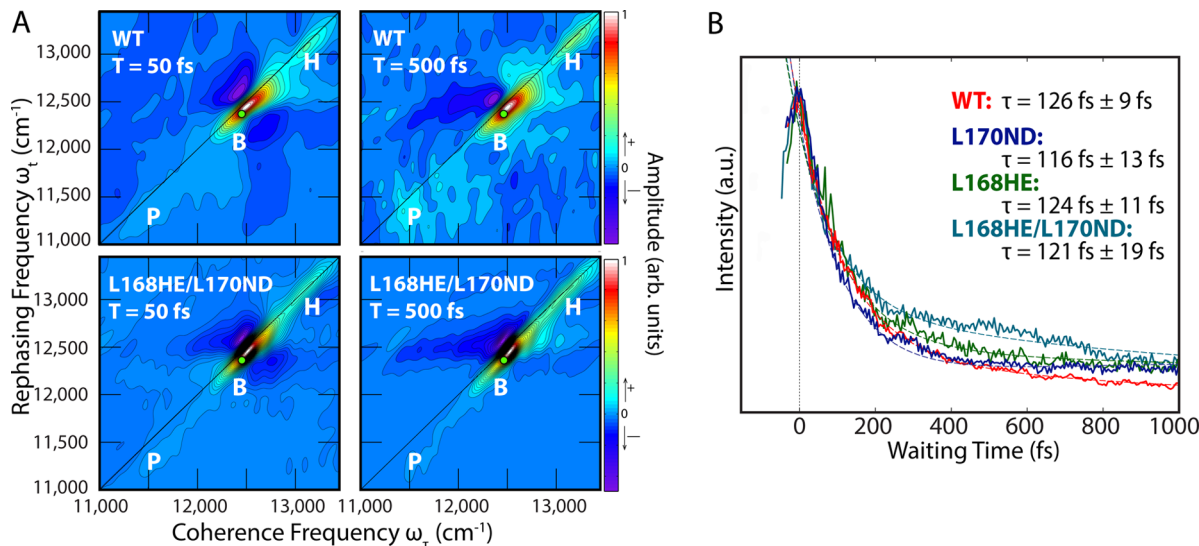


Figure 2. Rephasing 2DES and dynamics of mutant reaction centers. (A) Cryogenic rephasing 2D spectra of wild type and L168HE/L170ND mutant of the reaction center for waiting times $T = 50$ fs and $T = 500$ fs. The color map for each spectrum is normalized to the maximum of that spectrum. The green circle marks the location the traces in Figure 2b. (B) Waiting time traces of the B peak (green circle) for the WT and three mutants. Biexponential fits are shown as dashed lines for each waiting time trace. The dominant decay constant with one standard deviation is reported for each.

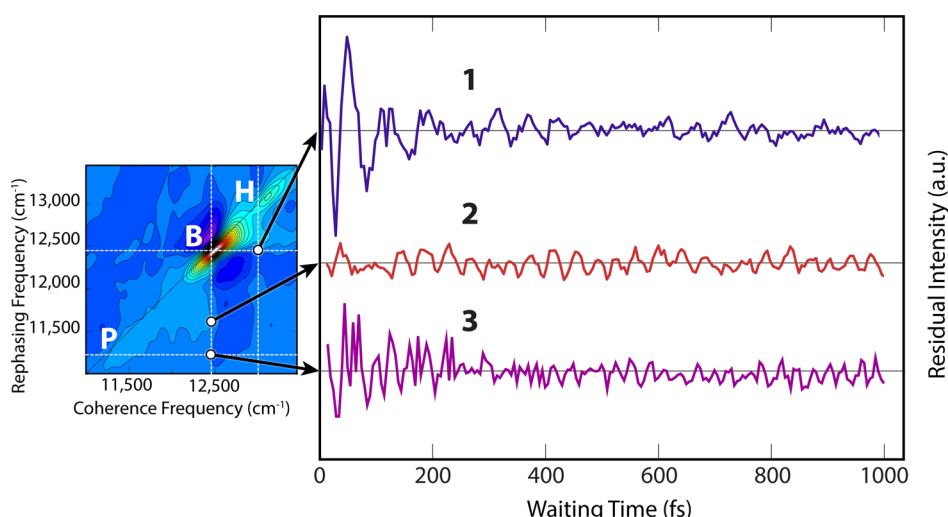


Figure 3. Coherence amplitude and decay rate enhancement at cross peak locations. Three traces in waiting time are taken from the wild-type 2D rephasing spectrum. Each trace is fit to a double-exponential plus offset function and the residuals are shown above exciton energies are highlighted with white dashed lines. Traces 1 and 3, which are located where an excitonic cross peak would be, begin with a higher amplitude that quickly decays. Trace 2 is from a purely vibrational mode coupled to the B exciton. All residual traces are plotted to scale.

Representative broadband rephasing 2DES data for the WT and L170ND/L168HE double mutant at 77 K are shown in Figure 2a. Each spectrum is phased to pump–probe data and shows the real component of the data normalized to its own maximum. The laser bandwidth was sufficient to cover the majority of the P peak in the blue-shifted mutants, but only the red side of the band in the WT. In these spectra, the B and H peaks are apparent as diagonally elongated peaks. This diagonal elongation clearly illustrates inhomogeneous broadening of these bands.³⁵ Pigment–protein complexes tend to be inhomogeneously broadened because the protein environments are relatively static compared to the time scale of our measurements. The low amplitude P peak in the double mutant spectra is consistent with the weak transition in the linear absorption and the lower intensity on the red edge of the

laser spectrum. The wild-type spectrum shows the P feature is much rounder than the other peaks, which is consistent with the P state having the shortest lifetime.

B. RC Coherences. Several groups have reported coherences between the B and H excitons in the reaction center at both cryogenic and room temperatures.^{6,22,36} However, the vibrational or electronic character of coherences across photosynthetic complexes is a subject of debate. Our data accesses the P exciton as well as the B and H, so we are able to compare coherence beating signals across a greater range of energies. In Figure 3, we show the beating at the B/H and B/P cross peaks (traces 1 and 3 respectively), as well as a location that is expected to be purely vibrational (trace 2). These are only representative traces. The entire data set is analyzed and the resultant beating maps of residual coherence

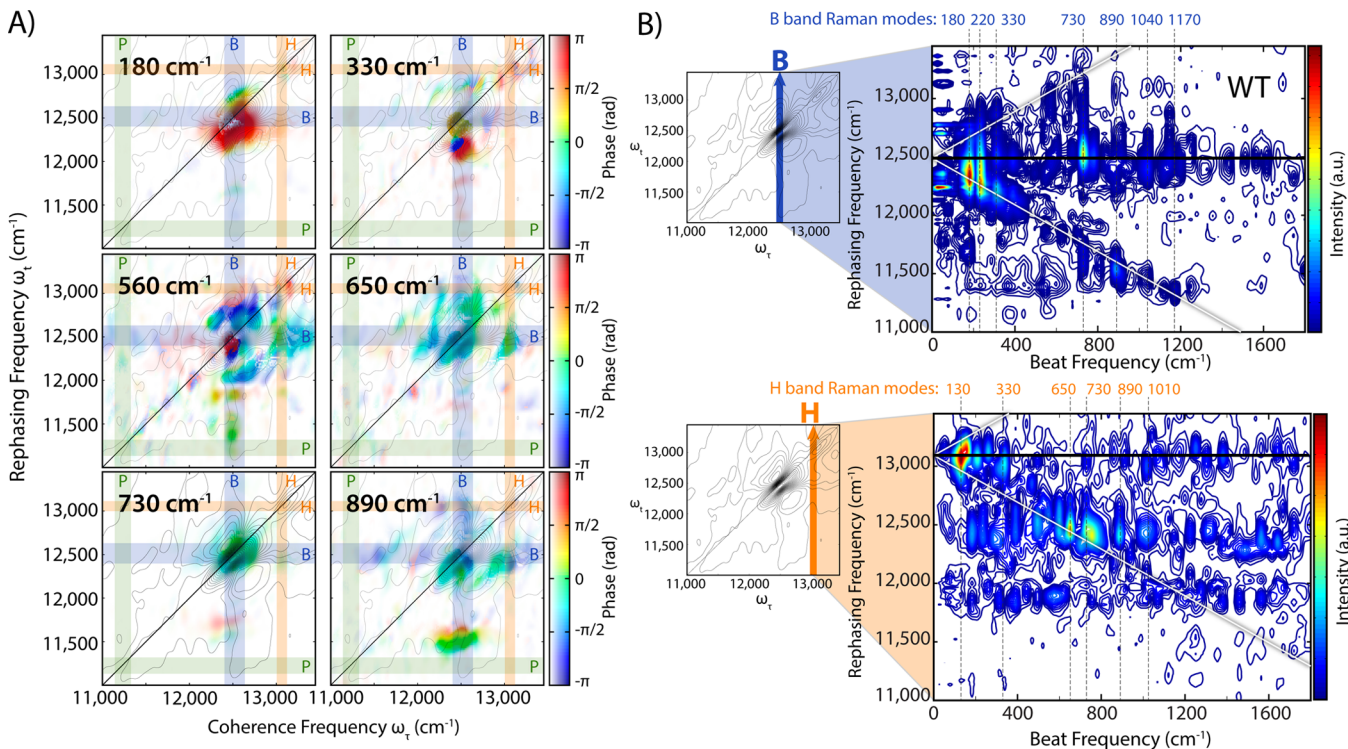


Figure 4. Power spectra reveal vibration–exciton coupling. (A) The Fourier magnitude and phase for six frequencies are plotted on the rephasing 2D map for some of the observed modes. The color of the heatmap indicates phase in radians, whereas the intensity of the peak corresponds to magnitude. Contour lines from the real part of the rephasing 2D spectra are shown to orient the reader. The transparent bars highlight energies of the P, B, and H exciton energies. Beatmaps showing only amplitude are shown in Figures S5 and S6 for clarity. (B) Power spectrum slices through rephasing frequencies at the B and H site energies for the wild-type reaction center. The solid black line in each spectrum indicates the energy that the slice was taken, whereas the white lines represent expected vibrational peak locations. Noticeably, the accessory bacteriochlorophyll B exciton exhibits a progression of vibrational modes that are discernible all the way to 1170 cm^{-1} .

signal are found in Figures 4, S5, and S6. The traces are the residual of the signal in the waiting time domain after a double-exponential fit is subtracted. Trace 2 shows a vibrational coherence associated with the accessory bacteriochlorophylls at a known Raman mode, 730 cm^{-1} . Both traces 1 and 3 not only exhibit an expected vibrational mode but also show an increased amplitude with a fast decay. We believe that the short-time, high-amplitude signals that decay rapidly arise from a different source than the vibrational modes that persist at long times in agreement with previous studies on the reaction center and photosynthetic coherences.^{9,17,22,24,25} Traces 1 and 3 both have two clear time components, a short time component and a long one. The large amplitude (3–5% of the signal) and fast decay in 100–200 fs in traces 1 and 3 are characteristic of electronic coherences, and the lower amplitude (1–2% of the signal) and long lifetime (greater than a picosecond) are characteristic of vibrational coherences. With spectroscopic data that includes excitation of more energetic vibrational modes, we can directly compare pure vibrational coherences and vibronic ones within the reaction center complex.

IV. DISCUSSION

A. Energy Transfer Dynamics. Energy transfer between H, B, and P has been documented previously in the literature.^{2–4,9} Typically, energy transfer appears in a 2D spectrum as an off-diagonal cross peak. Because the P peak has a relatively weak transition dipole and energy transfer from B to P is reported to be 115–200 fs,^{3,6,37,38} the cross peak is barely visible above the noise as an elongated shoulder on the lower

energy side of the B peak. Therefore, to look for differences in chromophore interactions, we need to extract the decay rates of the diagonal peaks in which the fast decay of B reveals population relaxation to P. A two-step global analysis was performed on the spectra to characterize the decay rates in the signal. In the first step each waiting time trace is fit to a double exponential with decay rates of 130 and 1000 fs plus an offset, based on rates reported in the literature.³ In the second step we fit the decay rates, allowing for variation in the rates so we can compare mutant complexes to the wild type. The resulting decay rate spectra³⁹ are shown in Figures S3 and representative traces from one point ($\omega_{\tau} = 12490\text{ cm}^{-1}$ and $\omega_t = 12470\text{ cm}^{-1}$) on the B peak are shown in Figure 2b. The data show very similar decay constants centered around 125 fs across all four mutants and across the diagonal length of the peak, indicating that population transfer from B to P is robust and homogeneous.

The primary sequence modifications in the mutant proteins were designed to be disruptive. Both mutations are very close to the special pair and introduce distinct electrostatic environments. Therefore, the robustness of these results across samples is surprising. For these amino acid changes, the resulting decay rates are all within the margin of error of our measurement. Energy transfer within this complex appears to be robust to mutation, and the protein scaffold is not delicately tuned to promote energy transfer. Interpreted through an evolutionary lens, this design makes sense: Biological systems are subject to constant perturbation and ideally, light harvesting should be insensitive to common mutations and external

influences.⁴⁰ We do not mean to say the protein has no impact on excited state dynamics, but only that these amino acid changes to environment do not manifest themselves as changes to transfer rates.

The observations are consistent with a few differing hypotheses. Either the protein environment has no effect on the excited state dynamics in this complex or the dynamics do rely on some aspect of coupling to the environment but the complex is built to withstand this large primary sequence perturbation. Considering that a protein is a relatively static and structured solvation environment and that extensive experimental evidence exists for electronic–vibrational coupling in pigment–protein complexes, we believe the first explanation is unlikely. Rather, we postulate that the complex's efficiency is well buffered against environmental changes. This hypothesis is consistent with prior results for the FMO complex.²⁹

In 2012, Kreisbeck and Kramer investigated the effect of different spectral densities on dynamics in the FMO complex.¹⁷ They found that the continuum component of the spectral density seems to greatly affect the dynamics; indeed, they only needed three explicit peaks in the function to reproduce FMO's behavior. This work suggests we can separate the bath into two components: the overdamped protein environment and a few underdamped vibrational frequencies. Chin et al. in 2013,^{25,44} Tiwari, Peters, and Jonas in 2013,⁴⁹ and Christensson et al. in 2012⁸ have come to similar conclusions regarding the distinction between intrapigment vibrations and the protein environment. Bacteriochlorophyll has a complex vibrational structure that has been extensively studied, so we next look to see if the vibrational structure in the excited state environment could help explain the persistence of fast and efficient transfer.^{10,14,41–43}

B. Vibrational Coupling. Recently, several groups have proposed vibronic models in which resonance and mixing between electronic energy gaps and vibrational modes are explicitly important in promoting the speed and efficiency of photosynthetic functions.^{15,18,21,22,27,44–48} The vibronic models propose some amount of mixing between the electronic and vibrational modes. If the vibrational contribution is included explicitly in the Hamiltonian, the result is a vibronic basis set defining states of the system. This can be used to explain energy differences and complicated excited state dynamics. Alternatively, the vibrational modes may be included as part of the bath. In this family of model, the vibration manifests as a peak in the spectral density function representing the bath, not the continuum. Both of these models are able to explain preserved and enhanced coherence signatures and energy transfer behavior, and they also depend on vibrational modes coupled to the electronic transition.

In Figure 3, we compare the residual beats from locations on the 2D map we expect to be pure vibrational coherences to residual beats from locations where an electronic coherence might occur (cross peak locations). In each of the cross peak residual traces, the frequency of the beat matched both the excitonic energy gap and the Raman mode expected at that location on the 2D map. However, at exciton cross peak locations the signal has two clear time components; it has increased amplitude and decay times under 200 fs (Traces 1 and 3 in Figure 3) and a component with a lifetime over 1000 fs. The long time component closely resembles purely vibrational signals seen in the data (Trace 2 in Figure 3). This long lifetime suggests some amount of vibrational–electronic mixing is responsible for the nature of the quantum

beats at cross peak locations and enhancing the signal at this frequency. In both Tiwari et al. and Chin et al. coherence enhancement and energy transport depend on the existence of a dominant vibrational mode resonant with the electronic transition.^{25,49} Therefore, we interpret the observation of enhanced coherences in our data as indirect evidence of the importance of an underdamped, resonant vibration coupled to the electronic states involved in excitonic energy transport. The frequency and dephasing time of these coherences depend on the environment, so we next use these coherences to investigate changes in the system–bath coupling when the protein is mutated.

Resonance Raman studies have shown that the different chromophores within the reaction center have different Raman spectra.^{5,10} Bacteriochlorophyll and bacteriopheophytin have many vibrational modes below 1200 cm⁻¹, the range accessible by our broadband laser pulse with excitation at 800 nm. Raman spectra from excitations of the B, P, and H bands show that some vibrational modes may be common to multiple excitons, but it is difficult to separate these modes to understand if they are delocalized modes or simply modes with similar frequencies. Indeed, each waiting time trace through the spectrum shows signatures of many beating frequencies. The relative enhancement of beating signals from the various vibrational modes is markedly different depending on the immediate environment.¹⁴ In the reaction center, the protein and the coupling provide very specific environments for the chromophores, so we expect the vibrations that couple to each exciton will not be identical. The vibrational spectrum within the 2DES spectra reveals which modes are enhanced in each exciton in this complex. Figure 4a presents the magnitude and phase of the known bacteriochlorophyll vibrational modes 180, 330, 560, 650, 730, and 890 cm⁻¹ mapped across the 2D spectra.^{7,19,41,42,50,51} Contour lines from the 2D spectrum are overlaid on the maps for clarity. The 730 and 890 cm⁻¹ modes show notable beating below the diagonal. In 2012, Butkus et al. theorize that vibrational cross peaks should beat out of phase with the diagonal peak, whereas cross peaks due to electronic coupling should be in phase with the diagonal peak. In experiments, many groups have reported phase shifts closer to $\pi/2$ radians in electronic coherences.^{6,23,24,52} Through this lens, the 730 cm⁻¹ mode below the B exciton is vibrational, and the 890 cm⁻¹ mode oscillates $\pi/2$ radians out of phase with the diagonal peak, indicating electronic origins. The 730 cm⁻¹ mode is clearly present on the H peak in addition to the B exciton. The 650 cm⁻¹ mode also appears on the H exciton. The lower energy modes are stronger in intensity, consistent with Raman studies.^{10,41,42} Consistent with previous reported data, the 180 cm⁻¹ mode is the strongest in both bacteriochlorophylls and bacteriopheophytins. Additionally, the 890 cm⁻¹ mode is stronger in the accessory bacteriochlorophylls and the 730 cm⁻¹ in both the B and H excitons, whereas the 650 cm⁻¹ mode is assigned to the bacteriopheophytins. These data lead us to conclude that the long-lived vibrational oscillations are properties of the pigments themselves, and not of the protein structure, in agreement with previous experiments.

In Figure 4b, the power spectra for vertical slices through the data sets are shown for both the H and B band. The top power spectrum slice at $\omega_\tau = 12\ 500\ \text{cm}^{-1}$ (Figure 4b, top) corresponds to the frequency of the B band and the lower power spectrum corresponds to the H band frequency, $\omega_\tau = 13\ 100\ \text{cm}^{-1}$ (Figure 4b, lower). The solid black line through

the power spectrum marks the rephasing frequency that equals the coherence frequency of the slice. In other words, data on the black line represent the power spectrum of the beating at the point where the slice crosses the main diagonal of the 2D spectrum. The solid white lines marks the region within the power spectrum where beating above/below the diagonal of the 2D spectrum matches the energy gap corresponding to the difference between the coherence and rephasing frequencies. For example, the 730 cm^{-1} beating feature below the diagonal peak in Figure 4a is the same as the contour peak at 730 cm^{-1} , 11770 cm^{-1} on the white line in the B band power spectrum (Figure 4b, upper). The dashed lines mark some of the expected modes from Cherepy et al.'s resonance Raman studies.⁴¹ In this spectrum, most of the prominent features fall on either the black or white lines.

Although the beating occurs throughout the spectrum, previous work has shown that vibrational and vibronic coherences appear primarily on the main diagonal as well as above, below and to the right of the diagonal peak on a rephasing two-dimensional spectrum.^{23,53–57} As shown in Figure 5, the power spectrum of the beating at every point

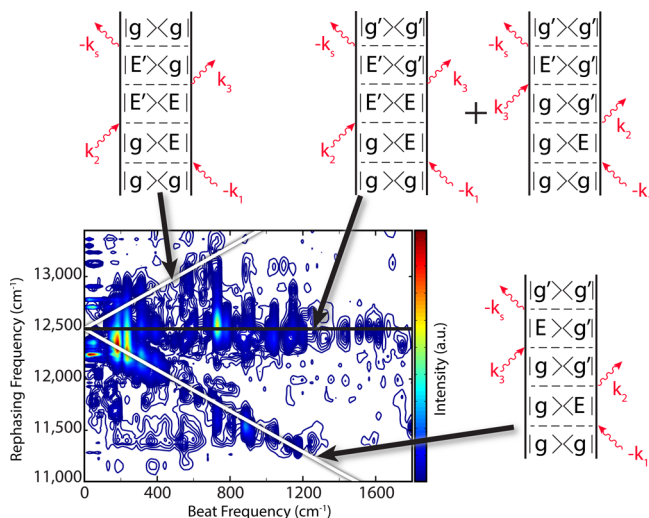


Figure 5. Feynman diagrams associated with beating within 2D rephasing spectra of the reaction center. The WT power spectra of beating along the B band from Figure 4 is reproduced here for clarity. The rephasing Feynman pathways that describe peaks that fall on each line are shown for the black and white lines. In these pathways, “g” is the ground state, “E” is an electronic excited state, and a prime, g' or E' indicates a hot vibrational state of energy ω on that electronic state.

along the $\omega_r = 12500\text{ cm}^{-1}$ (B band) slice shows beating arising from distinct rephasing Feynman diagrams. These diagrams assist in assigning beats to the ground and excited state surfaces as well as examining intensity patterns for signs of enhancement due to vibronic coupling. In fact, each Feynman pathway shown in Figure 5 contains exactly two transitions that involve a Franck–Condon factor leading to the simple hypothesis that the transitions should be equally strong. Instead, we observed stronger beating on the white line than on the black line when the vibrational mode is coincident with an electronic energy gap. To clarify this observation, the power spectrum along each on these lines is plotted in Figure 6 for the wild type and each mutant reaction center. The wild-type power spectrum corresponding to the black line in Figure 5 (B exciton) shows a strong mode at 730 cm^{-1} , but any modes at

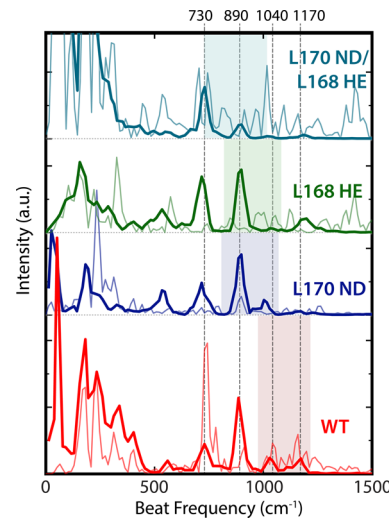


Figure 6. Power spectra of beating in mutant *R. sphaeroides* show changes in vibronic coupling with perturbations to P band transition energy. Two power spectrum slices are shown for each mutant reaction center. The fine lines show beating of the diagonal feature corresponding to the B exciton (equivalent to the horizontal black line in Figure 4). The thick lines are power spectra of beating below the B exciton where the beat frequency matches the gap between ω_r and ω_t (equivalent to the lower diagonal white line in Figure 4). The shading illustrates the energy gap in each wild type or mutant reaction center. Notably, the 730 cm^{-1} mode is present on the B exciton in the wild type, but missing in the mutant reaction centers. However, the mode is still strong at the cross peak location.

890 , 1040 , or 1180 cm^{-1} are indistinguishable from noise. However, the power spectrum from the lower white line in Figure 5 (the cross peak locations) shows clear peaks at 890 , 1040 , and 1170 cm^{-1} . The beating signatures can be affected by the laser excitation spectrum and compression.⁵⁸ The high energy vibrational modes are more dependent on the laser power at the edges of the spectrum. These spectra all result from excitation of the B exciton, but excitation of the vibrational modes and detection on the white line in Figure 5 greatly depend on the red edge of the spectrum. Therefore, definitive assignment of the mechanism requires further measurements, but the coincidence between the Raman modes and the excitonic energy gaps along with the enhanced amplitude of beating modes coincident with excitonic cross peaks strongly suggests a vibronic origin over purely vibrational or electronic beats.

The power spectra for the mutant RCs shown in Figure 6 support the theory of vibrational and electronic state mixing as well, and offer an explanation for the lack of change in energy transfer between mutants. Each of the mutant samples has a blue-shifted P peak relative to the WT, and therefore, a different excitonic energy difference between B and P. These mutants have the same vibrational progression below the B diagonal peak, but the higher frequency modes, 1040 and 1170 cm^{-1} , are weaker or missing, whereas the 730 and 890 cm^{-1} appears stronger in the power spectra. The power spectra follow the pattern set by the wild type; each of the peaks along the white line power spectrum that is resonant with the electronic transition is missing from the corresponding black line spectrum. However, the mutants do not have the 730 cm^{-1} peak in the black line spectrum that the wild type has, implying that the nature of the 730 cm^{-1} vibrations in the mutants is different from the wild type. This result is interesting because it

supports the view that coherence and fast energy transfer do depend on the existence of a vibrational mode that is resonant with the electronic energy gap. Bacteriochlorophyll has enough strong vibrational modes at low energies that the electronic transitions coupled to different vibrations in the mutants than in the wild type.

V. CONCLUSIONS

We perturbed the immediate environment around the special pair chromophores by point mutations to the protein in the vicinity. We do not observe significant changes in the energy transfer dynamics with these perturbations though we do observe large spectral changes. Therefore, we conclude that the primary structure of the protein is not finely tuned to promote energy transfer in the reaction center; this observation does not run counter to the evolutionary pressure on this complex for charge separation rather than light harvesting. In this complex, the protein simply provides the environment that determines each chromophore's site energy and coupling to other chromophores. In other words, the protein determines the excitonic energy gaps. As long as there is a vibrational mode degenerate with this energy gap, coherences and vibronic mixing appears to be enhanced. For example, when bacteriochlorophyll had vibrations that matched the new B/P energy gap in the mutant RCs and vibronic mixing occurred with the 730 and 890 cm^{-1} modes instead of the 1040 and 1170 cm^{-1} modes.

The mutants RCs explored in this study differ in one or two amino acids in close proximity to the special pair. The resulting dynamics prove to be robust to these mutations. Evolutionarily, this robustness could be an advantage because light harvesting would easily survive mutations to the genome. Alternatively, the evolutionary pressure on this complex is related to charge separation rather than energy transfer so it remains possible that such finely tuned mechanisms are operative but simply not in this complex. This persistence of B dynamics despite changes in the P exciton supports the notion that resonance between vibrational modes and excitonic energy differences is important in this fast energy transfer. The accessory bacteriochlorophylls exhibit a progression of strong vibrational modes from 730 to 1170 cm^{-1} meaning that it has the array of vibrational modes to resonate with a range of excitonic energy gaps. The chromophore itself is adaptable to changes in the exciton energies.

Bacteriochlorophyll on its own does not exhibit strong vibrational coherences in 2DES⁵⁹ but in a protein it shows a distinctive vibrational structure. In this study, we show a very clear map of which vibrations are enhanced in the reaction center, consistent with resonance Raman data in the literature.^{10,41–43} This map strikingly emphasizes that vibrations appear in the same locations as exciton cross peaks. A detailed analysis of the beats present on- and off-cross-peak locations reveals a fundamental difference in the nature of vibrational coherences when they coincide with an excitonic energy gap. At a cross peak location, these coherences clearly exhibit both electronic and vibrational characteristics. This coincidence significantly supports the vibronic hypothesis that it is the resonance and mixing between the two modes that prolongs the coherences. It is both the protein's effect on the site energy of each exciton and inherent properties in bacteriochlorophyll that contribute to this robust phenomenon in the bacterial reaction center.

■ ASSOCIATED CONTENT

■ Supporting Information

The Supporting Information is available free of charge on the ACS Publications website at DOI: 10.1021/acs.jpca.5b08366.

Further analysis and replicate data with different excitation and detection laser spectra are presented (PDF)

■ AUTHOR INFORMATION

Corresponding Author

*G. S. Engel. E-mail: gsengel@uchicago.edu.

Notes

The authors declare no competing financial interest.

■ ACKNOWLEDGMENTS

We thank JoAnn Williams for providing the WT and mutant bacterial strains. The authors also thank MRSEC (DMR 14-20709), the DARPA QuBE program (N66001-10-1-4060), AFSOR (FA9550-09-1-0117), the Camille and Henry Dreyfus Foundation, and the Searle Foundation for supporting the work in this publication. P.D.L. acknowledges support from the DOE-SCGF program. S.C.M. acknowledges support from the Department of Defense (DoD) through the National Defense Science & Engineering Graduate Fellowship (NDSEG) Program. P.D.D. acknowledges support from the NSF-GFRP program, and M.L.F. and P.D.D. were supported by the National Institute of Biomedical Imaging And Bioengineering of the National Institutes of Health under Award Number T32-EB009412.

■ REFERENCES

- (1) van Amerongen, H.; Valkunas, L.; van Grondelle, R. *Photosynthetic Excitons*; World Scientific: River Edge, NJ, 2000.
- (2) Arnett, D. C.; Moser, C. C.; Dutton, P. L.; Scherer, N. F. The First Events in Photosynthesis: Electronic Coupling and Energy Transfer Dynamics in the Photosynthetic Reaction Center from Rhodobacter Sphaeroides. *J. Phys. Chem. B* **1999**, *103*, 2014–2032.
- (3) Jordanides, X. J.; Scholes, G. D.; Fleming, G. R. The Mechanism of Energy Transfer in the Bacterial Photosynthetic Reaction Center. *J. Phys. Chem. B* **2001**, *105*, 1652–1669.
- (4) Parkinson, D. Y.; Lee, H.; Fleming, G. R. Measuring Electronic Coupling in the Reaction Center of Purple Photosynthetic Bacteria by Two-Color, Three-Pulse Photon Echo Peak Shift Spectroscopy. *J. Phys. Chem. B* **2007**, *111*, 7449–7456.
- (5) Scholes, G. D.; Fleming, G. R.; Olaya-Castro, A.; van Grondelle, R. Lessons from Nature About Solar Light Harvesting. *Nat. Chem.* **2011**, *3*, 763–774.
- (6) Lee, H.; Cheng, Y.-C.; Fleming, G. R. Coherence Dynamics in Photosynthesis: Protein Protection of Excitonic Coherence. *Science* **2007**, *316*, 1462–1465.
- (7) Turner, D. B.; Dinshaw, R.; Lee, K.-K.; Belsley, M. S.; Wilk, K. E.; Curmi, P. M. G.; Scholes, G. D. Quantitative Investigations of Quantum Coherence for a Light-Harvesting Protein at Conditions Simulating Photosynthesis. *Phys. Chem. Chem. Phys.* **2012**, *14*, 4857–4874.
- (8) Christensson, N.; Kauffmann, H. F.; Pullerits, T.; Mancal, T. Origin of Long-Lived Coherences in Light-Harvesting Complexes. *J. Phys. Chem. B* **2012**, *116*, 7449–7454.
- (9) Blankenship, R. E. *Molecular Mechanisms of Photosynthesis*; Blackwell Science: Oxford, Malden, MA, 2002.
- (10) Cherepy, N. J.; Shreve, A. P.; Moore, L. J.; Boxer, S. G.; Mathies, R. A. Electronic and Nuclear Dynamics of the Accessory Bacteriochlorophylls in Bacterial Photosynthetic Reaction Centers from Resonance Raman Intensities. *J. Phys. Chem. B* **1997**, *101*, 3250–3260.

- (11) Brixner, T.; Mancal, T.; Stiopkin, I. V.; Fleming, G. R. Phase-Stabilized Two-Dimensional Electronic Spectroscopy. *J. Chem. Phys.* **2004**, *121*, 4221–4236.
- (12) Cowan, M. L.; Ogilvie, J. P.; Miller, R. J. D. Two-Dimensional Spectroscopy Using Diffractive Optics Based Phased-Locked Photon Echoes. *Chem. Phys. Lett.* **2004**, *386*, 184–189.
- (13) Hybl, J. D.; Albrecht, A. W.; Faeder, S. M. G.; Jonas, D. M. Two-Dimensional Electronic Spectroscopy. *Chem. Phys. Lett.* **1998**, *297*, 307–313.
- (14) Arnett, D. C.; Yang, T.-S.; Scherer, N. F. Optical and Vibrational Coherence in Bacteriochlorophyll A. In *Time-Resolved Vib. Spectrosc., Proc. Int. Conf. TRVS*; Los Alamos National Labs: Santa Fe, NM, 1997; pp 131–135.
- (15) Chenu, A.; Christensson, N.; Kauffmann, H. F.; Mancal, T. Enhancement of Vibronic and Ground-State Vibrational Coherences in 2D Spectra of Photosynthetic Complexes. *Sci. Rep.* **2013**, *3*, 2029.
- (16) Engel, G. S.; Calhoun, T. R.; Read, E. L.; Ahn, T.-K.; Mancal, T.; Cheng, Y.-C.; Blankenship, R. E.; Fleming, G. R. Evidence for Wavelike Energy Transfer through Quantum Coherence in Photosynthetic Systems. *Nature* **2007**, *446*, 782–786.
- (17) Kreisbeck, C.; Kramer, T. Long-Lived Electronic Coherence in Dissipative Exciton Dynamics of Light-Harvesting Complexes. *J. Phys. Chem. Lett.* **2012**, *3*, 2828–2833.
- (18) Lim, J.; Palecek, D.; Caycedo-Soler, F.; Lincoln, C. N.; Prior, J.; von Berlepsch, H.; Huelga, S. F.; Plenio, M. B.; Zigmantas, D.; Hauer, J. Vibronic Origin of Long-Lived Coherence in an Artificial Molecular Light Harvester. *Nat. Commun.* **2015**, *6*, 7755.
- (19) Milota, F.; Prokhortenko, V. I.; Mancal, T.; von Berlepsch, H.; Bixner, O.; Kauffmann, H. F.; Hauer, J. Vibronic and Vibrational Coherences in Two-Dimensional Electronic Spectra of Supramolecular J-Aggregates. *J. Phys. Chem. A* **2013**, *117*, 6007–6014.
- (20) Plenio, M. B.; Almeida, J.; Huelga, S. F. Origin of Long-Lived Oscillations in 2D-Spectra of a Quantum Vibronic Model: Electronic Versus Vibrational Coherence. *J. Chem. Phys.* **2013**, *139*, 235102.
- (21) Romero, E.; Augulis, R.; Novoderezhkin, V. I.; Ferretti, M.; Thieme, J.; Zigmantas, D.; van Grondelle, R. Quantum Coherence in Photosynthesis for Efficient Solar-Energy Conversion. *Nat. Phys.* **2014**, *10*, 676–683.
- (22) Ryu, I. S.; Dong, H.; Fleming, G. R. Role of Electronic-Vibrational Mixing in Enhancing Vibrational Coherences in the Ground Electronic States of Photosynthetic Bacterial Reaction Center. *J. Phys. Chem. B* **2014**, *118*, 1381–1388.
- (23) Turner, D. B.; Wilk, K. E.; Curmi, P. M. G.; Scholes, G. D. Comparison of Electronic and Vibrational Coherence Measured by Two-Dimensional Electronic Spectroscopy. *J. Phys. Chem. Lett.* **2011**, *2*, 1904–1911.
- (24) Butkus, V.; Zigmantas, D.; Valkunas, L.; Abramavicius, D. Vibrational Vs. Electronic Coherences in 2D Spectrum of Molecular Systems. *Chem. Phys. Lett.* **2012**, *545*, 40–43.
- (25) Chin, A. W.; Prior, J.; Rosenbach, R.; Caycedo-Soler, F.; Huelga, S. F.; Plenio, M. B. The Role of Non-Equilibrium Vibrational Structures in Electronic Coherence and Recoherence in Pigment-Protein Complexes. *Nat. Phys.* **2013**, *9*, 113–118.
- (26) Butkus, V.; Valkunas, L.; Abramavicius, D. Vibronic Phenomena and Exciton-Vibrational Interference in Two-Dimensional Spectra of Molecular Aggregates. *J. Chem. Phys.* **2014**, *140*, 034306.
- (27) Fuller, F. D.; Pan, J.; Gelzinis, A.; Butkus, V.; Senlik, S. S.; Wilcox, D. E.; Yocom, C. F.; Valkunas, L.; Abramavicius, D.; Ogilvie, J. P. Vibronic Coherence in Oxygenic Photosynthesis. *Nat. Chem.* **2014**, *6*, 706–711.
- (28) Panitchayangkoon, G.; Hayes, D.; Fransted, K. A.; Caram, J. R.; Harel, E.; Wen, J. Z.; Blankenship, R. E.; Engel, G. S. Long-Lived Quantum Coherence in Photosynthetic Complexes at Physiological Temperature. *Proc. Natl. Acad. Sci. U. S. A.* **2010**, *107*, 12766–12770.
- (29) Hayes, D.; Wen, J.; Panitchayangkoon, G.; Blankenship, R. E.; Engel, G. S. Robustness of Electronic Coherence in the Fenna-Matthews-Olson Complex to Vibronic and Structural Modifications. *Faraday Discuss.* **2011**, *150*, 459–469.
- (30) Goldsmith, J. O.; Boxer, S. G. Rapid Isolation of Bacterial Photosynthetic Reaction Centers with an Engineered Poly-Histidine Tag. *Biochim. Biophys. Acta, Bioenerg.* **1996**, *1276*, 171–175.
- (31) Zheng, H. B.; Caram, J. R.; Dahlberg, P. D.; Rolczynski, B. S.; Viswanathan, S.; Dolzhnikov, D. S.; Khadivi, A.; Talapin, D. V.; Engel, G. S. Dispersion-Free Continuum Two-Dimensional Electronic Spectrometer. *Appl. Opt.* **2014**, *53*, 1909–1917.
- (32) Caram, J. R.; Zheng, H. B.; Dahlberg, P. D.; Rolczynski, B. S.; Griffin, G. B.; Dolzhnikov, D. S.; Talapin, D. V.; Engel, G. S. Exploring Size and State Dynamics in Cdse Quantum Dots Using Two-Dimensional Electronic Spectroscopy. *J. Chem. Phys.* **2014**, *140*, 084701.
- (33) Singh, V. P.; Fidler, A. F.; Rolczynski, B. S.; Engel, G. S. Independent Phasing of Rephasing and Non-Rephasing 2D Electronic Spectra. *J. Chem. Phys.* **2013**, *139*, 084201.
- (34) Williams, J. C.; Haffa, A. L. M.; McCulley, J. L.; Woodbury, N. W.; Allen, J. P. Electrostatic Interactions between Charged Amino Acid Residues and the Bacteriochlorophyll Dimer in Reaction Centers from Rhodobacter Sphaeroides. *Biochemistry* **2001**, *40*, 15403–15407.
- (35) Cho, M. H.; Brixner, T.; Stiopkin, I.; Vaswani, H.; Fleming, G. R. Two Dimensional Electronic Spectroscopy of Molecular Complexes. *J. Chin. Chem. Soc.* **2006**, *53*, 15–24.
- (36) Westenhoff, S.; Paleček, D.; Edlund, P.; Smith, P.; Zigmantas, D. Coherent Picosecond Exciton Dynamics in a Photosynthetic Reaction Center. *J. Am. Chem. Soc.* **2012**, *134*, 16484–16487.
- (37) Jia, Y.; Jonas, D. M.; Joo, T.; Nagasawa, Y.; Lang, M. J.; Fleming, G. R. Observation of Ultrafast Energy Transfer from the Accessory Bacteriochlorophylls to the Special Pair in Photosynthetic Reaction Centers. *J. Phys. Chem.* **1995**, *99*, 6263–6266.
- (38) Vos, M. H.; Breton, J.; Martin, J.-L. Electronic Energy Transfer within the Hexamer Cofactor System of Bacterial Reaction Centers. *J. Phys. Chem. B* **1997**, *101*, 9820–9832.
- (39) Myers, J. A.; Lewis, K. L. M.; Fuller, F. D.; Tekavec, P. F.; Yocom, C. F.; Ogilvie, J. P. Two-Dimensional Electronic Spectroscopy of the D1-D2-Cyt B559 Photosystem II Reaction Center Complex. *J. Phys. Chem. Lett.* **2010**, *1*, 2774–2780.
- (40) Kramer, T.; Kreisbeck, C. In *Modelling Excitonic-Energy Transfer in Light-Harvesting Complexes*; AIP Conference Proceedings; AIP: Melville, NY, 2014.
- (41) Cherepy, N. J.; Shreve, A. P.; Moore, L. J.; Boxer, S. G.; Mathies, R. A. Temperature Dependence of the Qy Resonance Raman Spectra of Bacteriochlorophylls, the Primary Electron Donor, and Bacteriopheophytins in the Bacterial Photosynthetic Reaction Center. *Biochemistry* **1997**, *36*, 8559–8566.
- (42) Cherepy, N. J.; Shreve, A. P.; Moore, L. J.; Franzen, S.; Boxer, S. G.; Mathies, R. A. Near-Infrared Resonance Raman-Spectroscopy of the Special Pair and the Accessory Bacteriochlorophylls in Photosynthetic Reaction Centers. *J. Phys. Chem.* **1994**, *98*, 6023–6029.
- (43) Shreve, A. P.; Cherepy, N. J.; Franzen, S.; Boxer, S. G.; Mathies, R. A. Rapid-Flow Resonance Raman-Spectroscopy of Bacterial Photosynthetic Reaction Centers. *Proc. Natl. Acad. Sci. U. S. A.* **1991**, *88*, 11207–11211.
- (44) del Rey, M.; Chin, A. W.; Huelga, S. F.; Plenio, M. B. Exploiting Structured Environments for Efficient Energy Transfer: The Phonon Antenna Mechanism. *J. Phys. Chem. Lett.* **2013**, *4*, 903–907.
- (45) Sato, Y.; Doolittle, B. Influence of Intra-Pigment Vibrations on Dynamics of Photosynthetic Exciton. *J. Chem. Phys.* **2014**, *141*, 185102.
- (46) Perlik, V.; Seibt, J.; Cranston, L. J.; Cogdell, R. J.; Lincoln, C. N.; Savolainen, J.; Sanda, F.; Mancal, T.; Hauer, J. Vibronic Coupling Explains the Ultrafast Carotenoid-to-Bacteriochlorophyll Energy Transfer in Natural and Artificial Light Harvesters. *J. Chem. Phys.* **2015**, *142*, 212434.
- (47) Womick, J. M.; West, B.; Scherer, N. F.; Moran, A. M. Vibronic Effects in the Spectroscopy and Dynamics of C-Phycocyanin. *J. Phys. B: At., Mol. Opt. Phys.* **2012**, *45*, 154016.
- (48) Womick, J. M.; Moran, A. M. Vibronic Enhancement of Exciton Sizes and Energy Transport in Photosynthetic Complexes. *J. Phys. Chem. B* **2011**, *115*, 1347–1356.

- (49) Tiwari, V.; Peters, W. K.; Jonas, D. M. Electronic Resonance with Anticorrelated Pigment Vibrations Drives Photosynthetic Energy Transfer Outside the Adiabatic Framework. *Proc. Natl. Acad. Sci. U. S. A.* **2013**, *110*, 1203–1208.
- (50) Seibt, J.; Pullerits, T. Beating Signals in 2D Spectroscopy: Electronic or Nuclear Coherences? Application to a Quantum Dot Model System. *J. Phys. Chem. C* **2013**, *117*, 18728–18737.
- (51) Dostal, J.; Mancal, T.; Vacha, F.; Psencik, J.; Zigmantas, D. Unraveling the Nature of Coherent Beatings in Chlorosomes. *J. Chem. Phys.* **2014**, *140*, 115103.
- (52) Panitchayangkoon, G.; Voronine, D. V.; Abramavicius, D.; Caram, J. R.; Lewis, N. H. C.; Mukamel, S.; Engel, G. S. Direct Evidence of Quantum Transport in Photosynthetic Light-Harvesting Complexes. *Proc. Natl. Acad. Sci. U. S. A.* **2011**, *108*, 20908–20912.
- (53) Tekavec, P. E.; Myers, J. A.; Lewis, K. L. M.; Ogilvie, J. P. Two-Dimensional Electronic Spectroscopy with a Continuum Probe. *Opt. Lett.* **2009**, *34*, 1390–1392.
- (54) Caram, J. R.; Fidler, A. F.; Engel, G. S. Excited and Ground State Vibrational Dynamics Revealed by Two-Dimensional Electronic Spectroscopy. *J. Chem. Phys.* **2012**, *137*, 024507.
- (55) Senlik, S. S.; Policht, V. R.; Ogilvie, J. P. Two-Color Nonlinear Spectroscopy for the Rapid Acquisition of Coherent Dynamics. *J. Phys. Chem. Lett.* **2015**, *6*, 2413–20.
- (56) Egorova, D.; Gelin, M. F.; Domcke, W. Analysis of Cross Peaks in Two-Dimensional Electronic Photon-Echo Spectroscopy for Simple Models with Vibrations and Dissipation. *J. Chem. Phys.* **2007**, *126*, 074314.
- (57) Faeder, S. M. G.; Jonas, D. M. Two-Dimensional Electronic Correlation and Relaxation Spectra: Theory and Model Calculations. *J. Phys. Chem. A* **1999**, *103*, 10489–10505.
- (58) Bardeen, C. J.; Wang, Q.; Shank, C. V. Selective Excitation of Vibrational Wave-Packet Motion Using Chirped Pulses. *Phys. Rev. Lett.* **1995**, *75*, 3410–3413.
- (59) Fransted, K. A.; Caram, J. R.; Hayes, D.; Engel, G. S. Two-Dimensional Electronic Spectroscopy of Bacteriochlorophyll a in Solution: Elucidating the Coherence Dynamics of the Fenna-Matthews-Olson Complex Using Its Chromophore as a Control. *J. Chem. Phys.* **2012**, *137*, 125101.